Passive Stability of Stance is Determined by the Relationship Between Natural Frequency and Walking Frequency

Shane Riddle[1(✉)], Gregory Sutton[2], Victoria A. Webster-Wood[3], Hillel J. Chiel[4], and Roger D. Quinn[1]

[1] Department of Mechanical and Aerospace Engineering, Case Western Reserve University, Cleveland, OH 44106, USA
shane.riddle@case.edu
[2] School of Life Sciences, University of Lincoln (UK), LN6, 7TS, UK
[3] Department of Mechanical Engineering, Carnegie Mellon University, Pittsburgh, PA 15213, USA
[4] Department of Biology, Case Western Reserve University, Cleveland, OH 44106, USA

Abstract. The passive dynamics of stance can explain why large animals, like horses and humans, require neuromuscular activity to maintain stance whereas smaller animals like cockroaches do not [20]. The dynamic properties that govern an animal's movement, like inertia, stiffness, and damping, are dictated by its size, scaling with its length [28]. The natural frequency of an animal's limb in stance can be predicted using its stiffness to inertia ratio, which scales inversely with length. We theorize that the passive mechanics of smaller animal limbs, with higher resonant frequencies than walking cycle frequencies, restore limb position quickly enough that neuromuscular intervention is not needed to correct perturbations during stance. Larger animals, however, require muscle activation since their mechanics depend more on inertia and are less dominated by viscoelastic effects, leading to a lower natural frequency.

Keywords: Scaling · Stance · Passive Stability · Resonant Frequency.

1 Introduction

Regardless of size, the movements of all legged animals are governed by the same forces: inertia, gravity, stiffness, and damping. Scale, however, affects which of these influences locomotion dynamics the most. Recent studies suggest that locomotion behaviors can be split into three categories (kinetic, viscous, and quasi-static) based on limb length and walking cycle period [28]. Sutton et al. state that the differences in each behavior manifest in the phase shift between

This work was supported by NSF DBI 2015317 as part of the NSF/CIHR/DFG/FRQ/UKRI-MRC Next Generation Networks for Neuroscience Program

N. S. Szczecinski et al. (Eds.): Living Machines 2024, LNAI 14930, pp. 439–451, 2025.
https://doi.org/10.1007/978-3-031-72597-5_30

a joint's actuation and its displacement. A joint's rotational position (θ) can be described using a sinusoid while its velocity ($\dot{\theta}$) and acceleration ($\ddot{\theta}$) are the first and second time derivatives of its position. Each time derivative of a sinusoid shifts behavior 90° further out of phase. This means the actuation of a viscous system, largely dominated by velocity-dependent effects like damping, is 90° out of phase from joint motion. Similarly, a kinetic system, dominated by acceleration effects like inertia, is 180° out of phase. How do we categorize animals into these three regions?

An animal's size is the biggest contributing factor to its dynamic behavior. Because of the square-cube law, the mass of a given animal scales in accordance with its length cubed. At the same time, the linear stiffness and damping of an animal's joint muscles scale proportionally to its length [28]. This means the ratio of damping and stiffness to inertia is high for smaller animals and low for larger animals. As a consequence, the limbs of small creatures, like insects, are largely dominated by viscous and elastic forces, whereas the limbs of larger creatures like humans and horses are dominated by kinetic forces. The ratio of stiffness to inertia determines the natural frequency (Eq. (1)).

$$\omega_{\mathrm{n}} = \sqrt{\frac{k}{m}} \tag{1}$$

Given how mass (m) and stiffness (k) scale with size, the natural frequency (ω_{n}) will be higher for smaller animals and lower for larger animals.

When a non-periodic perturbation is applied to a passive dynamic system, it oscillates at its natural frequency. Animals, however, are not passive systems since they are capable of generating torques about their joints using their muscles. Many investigators have studied how animal locomotion and stance stability are affected by perturbations *in vivo* and in simulation [2,5,23,26,29,30]. A prevalent focus of these studies is how the nervous system controls the muscles to perform corrective actions accounting for perturbations. Bingham et al., for example, discuss that while a wider stance is commonly accepted as more stable for humans, this is actually due to the mechanical advantage wider stances offer neuromuscular control for torque generation as opposed to inherent mechanical stability [2]. On the other end of the spectrum, Jindrich et al. have shown that insects, like cockroaches, are passively stable; they do not need any neuromuscular interference to remain standing [20].

In this paper, we explore the interplay between animal size and passive stability in stance. We theorize that the need for corrective neuromuscular interference depends on the difference between an animal system's natural frequency and the frequency of its locomotion cycle. From literature, it is known that walking cycle frequency tends to scale inversely with animal size [3,10,11,15,16,18,19,34] and we have established that the same is true for animal natural frequencies while in stance. In particular, we expect walking frequencies to scale with $\frac{1}{\mathrm{length}^{0.35}}$, per Hooper 2012 [17], while resonant frequencies should scale with $\frac{1}{\mathrm{length}}$ per Eq. (1) and Sutton et al. 2023 [28]. The different scaling coefficients for these two values

mean that animals of different sizes have different relationships between resonant frequency and walking frequency.

We believe that the point at which natural frequency is overtaken by walking cycle frequency is when neuromuscular intervention is required to stabilize the system: the passive mechanics of the limb will restore limb position at the limb's natural resonant frequency, and if this frequency is very high, as it is in small insects, the speed of this reaction can be sufficiently fast that the nervous system will have no need to add additional torque. This would explain why larger animals require muscle activation to remain standing while smaller insects can do so passively [20]. Unlike cockroaches and fruit flies, kinetic force dominated animals on the scale of horses and humans have such low stiffness and damping compared to their mass that they cannot recover passively within one period of their walking cycle. This means they are liable to become unstable and potentially fall over during the walking cycle when perturbed unless they use their muscles to provide active stabilization.

2 Methods

To test this theory, we first constructed a mathematical inverted pendulum model of a leg in stance. We then used this to guide our modification of the 4-bar mechanism presented by Bingham et al., which mimics the standing position of a human [2]. This model is scalable so that we can import the mass and length of an animal to obtain an isometrically scaled human stance analog for that animal's size.

2.1 Inverted Pendulum

One of the simplest ways to represent the dynamics of a leg in stance is with an inverted pendulum spring-mass-damper system with the point of ground contact fixed via a pin joint. The general equation of motion for a rotational system, such as this, can be expressed as:

$$T = J\ddot{\theta} + c\dot{\theta} + k\theta \tag{2}$$

where J is inertia, c is rotational damping, and k is rotational stiffness. This study is interested in the leg's passive response when a perturbation is experienced during the stance phase. To this end, we considered the response of the inverted pendulum for an impulse of magnitude A applied at the hip, which can be modeled using the following textbook solution [24], which is based on impulse-momentum:

$$\theta(t) = \frac{A}{\sqrt{kJ}\sqrt{1-\left(\frac{c}{2J\omega_n}\right)^2}} e^{\left(\frac{-ct}{2J}\right)} \sin\left(\omega_n \sqrt{1-\left(\frac{c}{2J\omega_n}\right)^2} t\right) \tag{3}$$

The hip was chosen to replicate the force application site of the Stanford Bump'em system, a perturbation apparatus used to analyze human locomotion stability [29].

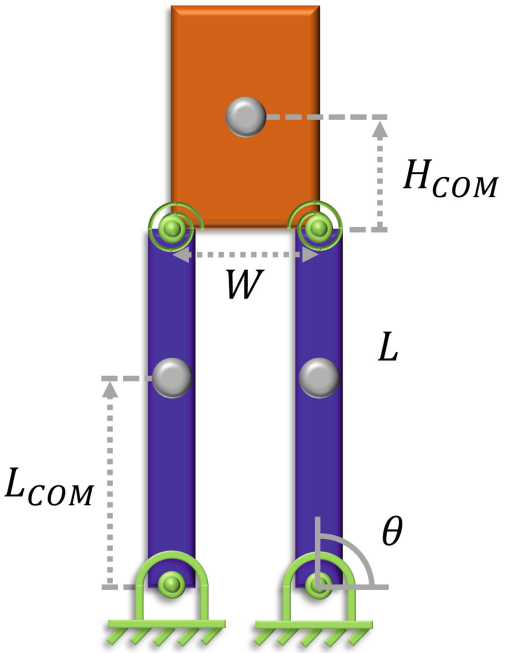

Fig. 1. The 4-bar model, modified from Bingham et al. 2011 [2]. The center of mass for each linkage is denoted by a gray circle and the hip torsion spring and dampers are denoted by the green spirals at the top of each leg. (Colour figure online)

2.2 Modified 4-Bar Model

While useful for analyzing the general motion of a leg, the inverted pendulum relies on the stiffness and damping of a joint between the leg and the ground, a joint that, anatomically speaking, does not exist. To create a more accurate stance model, we developed a dynamic model in Simscape, a Simulink (MATLAB) add-on package, similar to the 4-bar model presented in Bingham et al. 2011 [2]. The 4-bar consists of two pin joints at the ankles fixed to the ground and two pin joints at the hips with a leg link running from ankle to hip on each side and a torso link spanning the hip joints (Fig. 1).

The Bingham model implemented motors at the hip joints to study the effects of neuromuscular hip torque feedback on balance. We replaced these with torsional springs and dampers to emulate the passive dynamic properties of a hip joint. The stiffness and damping parameters were tuned in accordance with Sutton et al. [28], where rotational stiffness and damping for each hip can be calculated using leg length as:

$$k_{\mathrm{r}} = \frac{n}{2} k_0 s^2 L^3 \tag{4}$$

$$c_{\mathrm{r}} = \frac{n}{2} c_0 s^2 L^3 \tag{5}$$

where k_0 ($12{\cdot}10^3 \frac{N}{m^2}$, [18,27]) and c_0 ($1.31{\cdot}10^3 \frac{Ns}{m^2}$, [7,13,27,31,35]) are empirically determined proportionality constants and s ($10^{-1.5}$, [6,9,12,32]) is a unitless lever arm coefficient [28]. To allow this model to approximate stance for 6-legged insects, 4-legged mammals, and 2-legged humans, we lump the joint and leg properties of ipsilateral limbs. This means that each leg of the model actually represents half the number of legs (n) of the given animal. For a human with two legs, each hip model only contains one leg's worth of stiffness ($\frac{n}{2} = 1$), but for a fruit fly with six legs, each hip model has three legs worth of stiffness ($\frac{n}{2} = 3$). This simplification was made so that the effect of scale for the range of models tested could be explored using a single, approximate model.

Mass, inertia, and center of mass (COM) parameters were kept roughly the same as the Bingham model except for the distribution of mass between the legs (m_{leg}) and the trunk (m_{trunk}). The portion of the mass in all of the legs combined was changed from 32% of the total body mass to 25%, that of a rat [33]. Larger animals have a greater proportion of their mass in their legs compared to smaller species, like insects. To accommodate this, and generalize the model for the variety of animals analyzed, the rat mass distribution was used as it lies in the middle of the length scale of the species included in this study. The equations for all of the model parameters can be found in Table 1. Importantly, all of these parameters can be calculated with just two properties: effective leg length (L) and total body mass (m_{tot}). Both of these are somewhat commonly reported data points, allowing us to test this model for a wide variety of animals.

Table 1. The calculations for the parameters of the 4-bar model, using only body mass (m_{tot}) and leg length (L).

Model Parameter	Calculation
Leg Length [m]	L - From Literature
Total Body Mass [kg]	m_{tot} - From Literature
Total Body Length [m]	$L_{\text{tot}} = \frac{L}{0.530}$
Leg Mass [kg]	$m_{\text{leg}} = 0.125 * m_{\text{tot}}$
Leg Inertia about COM [kg m^2]	$I_{\text{leg}} = 0.030 * m_{\text{tot}} * L_{\text{tot}}$
Leg COM from ankle [m]	$L_{\text{COM}} = 0.293 * L_{\text{tot}}$
Trunk Mass [kg]	$m_{\text{trunk}} = 0.75 * m_{\text{tot}}$
Trunk Inertia about COM [kg m^2]	$I_{\text{leg}} = 0.020 * m_{\text{tot}} * L_{\text{tot}}$
Trunk COM from hip [m]	$H_{\text{COM}} = 0.108 * L_{\text{tot}}$
Hip Width [m]	$W = 0.134 * L_{\text{tot}}$

As for the perturbation, a linear force impulse was applied at the left hip of the 4-bar linkage to emulate the Stanford Bump'em, which applies sudden perturbation to subjects about the hip [29]. An impulse can be expressed in units of Force · time, which can be expanded to mass · acceleration · time, which has units of $\frac{\text{length}^4}{\text{time}}$. To accommodate this, the magnitude of the pulse was scaled

with L^4. As the Bump'em can apply up to 200 N of force for a human, the scaled force magnitude for other species was calculated as follows:

$$F_{\text{impulse}} = 200(\frac{L}{L_{\text{human}}})^4\text{N} \tag{6}$$

Since the leg length of an average human is roughly 1 m this reduces to $200L^4$N, where L is the animal leg length given in meters.

2.3 Animal Data

Animal masses and leg lengths were gathered from the literature and compiled in Table 2. The test animals included: horse, human, cat, rat, mouse, cockroach, and fruit fly. These cover leg lengths from 5 mm to 1.5 m, a range of 4 orders of magnitude. A table containing the walking cycle period of each animal was found in the supplementary documentation of Sutton et al. 2023 [28]. These values were converted to walking cycle frequency, with units $[\frac{\text{rad}}{\text{s}}]$, via the relationship $\omega = \frac{2\pi}{T}$ and recompiled into Table 2 here.

Table 2. The masses, lengths, and walking cycle frequencies gathered from the literature for the species of interest in this paper.

Species	Leg Length [m]	Body Mass [kg]	Walking Frequency $[\frac{\text{rad}}{\text{s}}]$	Refs
Horse	$1.5 \cdot 10^0$	$5.0 \cdot 10^2$	$7.1 \cdot 10^0$	[16,18]
Human	$1.0 \cdot 10^0$	$7.0 \cdot 10^1$	$1.3 \cdot 10^1$	[2,11]
Cat	$2.5 \cdot 10^{-1}$	$4.5 \cdot 10^0$	$2.5 \cdot 10^1$	[1,10]
Rat	$5.0 \cdot 10^{-2}$	$5.0 \cdot 10^{-1}$	$3.1 \cdot 10^1$	[8,19]
Mouse	$2.0 \cdot 10^{-2}$	$2.6 \cdot 10^{-2}$	$6.3 \cdot 10^1$	[4,15]
Cockroach	$8.0 \cdot 10^{-3}$	$1.0 \cdot 10^{-3}$	$1.4 \cdot 10^2$	[3,20]
Fruit Fly	$5.0 \cdot 10^{-4}$	$1.0 \cdot 10^{-7}$	$1.3 \cdot 10^2$	[25,34]

3 Results

To find the natural frequency (ω_n) of the 4-bar system for each animal, the perturbation simulation was run with each set of parameters neglecting damping terms. The position of the torso center of mass was recorded at each timestep and the peak-to-peak times of the resulting oscillations were calculated, giving us the period of oscillation (T) for the system. This was then converted into natural frequency, with units $[\frac{\text{rad}}{\text{s}}]$, the same way the walking frequencies were calculated. These frequencies, along with the walking cycle frequencies, were plotted against leg length in Fig. 2. This shows that the natural frequency scales inversely with animal leg length.

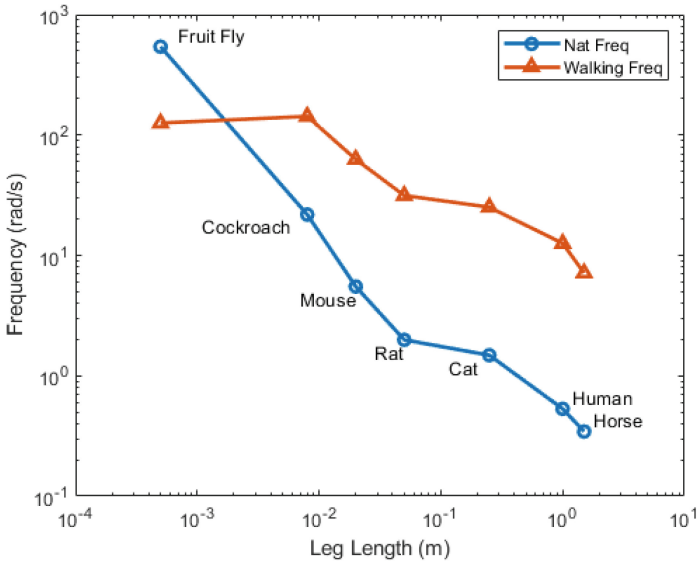

Fig. 2. The natural frequencies of the 4-bar model (blue) and walking cycle frequencies from literature (orange), as they scale with animal mass and leg length. (Colour figure online)

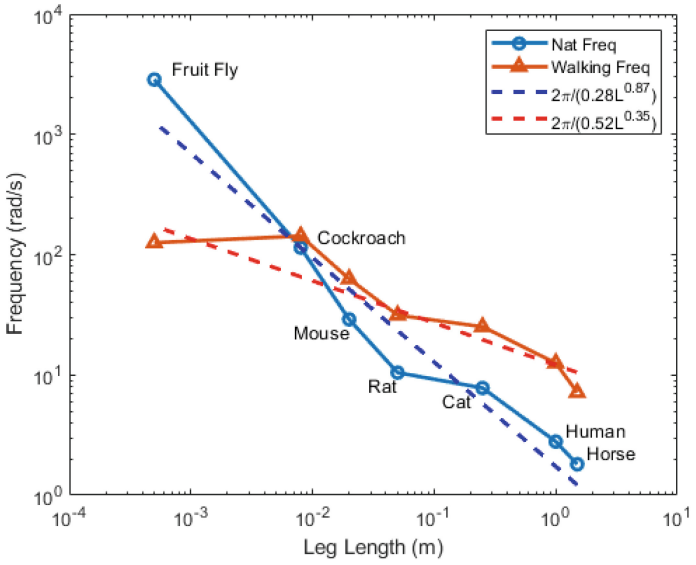

Fig. 3. Corrected natural frequencies of the 4-bar model (blue) and walking cycle frequencies (orange). Relation between walking frequency and length from Hooper 2012 [17] (red dashed line), and the linear regression of our data (blue dashed line) are also plotted. (Colour figure online)

From these results, it is apparent that the natural frequencies gathered from the model are smaller than the walking cycle frequencies for every animal, except for the fruit fly. This was unexpected given that we know, at the very least, that cockroaches possess passively stable stances [20]. To understand this discrepancy, we compared the stiffness of our model cockroach to that of a live cockroach. Jindrich et al. found the linear stiffness of a cockroach to be 16 $\frac{\mathrm{N}}{\mathrm{m}}$ [20] while our model parameters calculate a torsional stiffness of $5.1 \cdot 10^{-4}$ $\frac{\mathrm{Nm}}{\mathrm{rad}}$ for a single hip joint. We know from Sutton et al. that linear stiffness scales with L while rotational stiffness scales with L^3, so we divide our rotational stiffness by L^2 ($L = 8$ mm), giving us an equivalent linear stiffness of 0.29 $\frac{\mathrm{N}}{\mathrm{m}}$ per modeled hip, or 0.58 $\frac{\mathrm{N}}{\mathrm{m}}$ total. This means our 4-bar model may underestimate hip joint stiffness for the cockroach by a factor of 28.

To assess if this underestimation is responsible for the discrepancy between natural and walking frequency, we scaled all of our hip stiffnesses by a factor of 28 and re-ran the simulations. The results in Fig. 3 show that the lines now cross as expected, with the cockroach having a higher natural frequency than walking cycle frequency with the inflection point near the mouse scale (10^{-2} m). Also plotted in Fig. 3 is the trendline corresponding to walking frequency as a function of length, presented in Hooper 2012 [17]. Hooper states that the walking frequency of an animal scales with $\frac{1}{L^{0.35}}$, which agrees with the frequencies we found in the literature. While all animals are capable of a range of walking speeds, we considered only the maximum walking speeds reported in the literature for this analysis, as these closely aligned with the Hooper trendline. To estimate how our model's natural frequencies scaled with leg length, we performed a linear regression on the log-scaled data. This gave us Eq. (7) with a fraction of variance explained of $\mathrm{R}^2 = 0.95$.

$$\omega_{\mathrm{n}} = \frac{2\pi}{0.28L^{0.87}} \tag{7}$$

Equation (7) suggests that the natural frequency of our model scales with $\frac{1}{L^{0.87}}$. This deviates from the $\frac{1}{L}$ scaling we predicted based on Eq. (1) and Sutton et al. 2023 [28].

4 Discussion

To understand why the resonant frequency of our model does not scale as predicted, we consider the equation for the natural frequency of a rotational system:

$$\omega_{\mathrm{n}} = \sqrt{\frac{k_{\mathrm{r}}}{J}} \tag{8}$$

where torsional stiffness k_{r} and inertia J are expected to scale with L^3 and L^5 respectively [28]. We deduced that if the natural frequency was not scaling as expected, it was because at least one of these model properties was not scaling as expected. To test this, we reintroduced damping to the model and ran

the simulations again. This time, we used a constant force, scaled with L^4 as before, applied at the same location as the impulse, and recorded the steady state angular displacement of the system from rest with respect to the ankle $\Delta\theta$. The equation for the moment generated by a torsion spring is:

$$M = k_{\mathrm{r}} \cdot \Delta\theta \tag{9}$$

so, to find the stiffness of the whole model k_{r} we took the applied force multiplied by the leg length squared, to calculate the applied moment M, and divided by the recorded $\Delta\theta$. We then ran a linear regression on the log-scaled stiffnesses and found that the measured k_{r} scales with $L^{2.9}$, which is reasonably close to the expected L^3 scaling.

With stiffness scaling as expected, the discrepancy must lie in the inertia. Breaking J down further, we see it is not actually an independent variable, but rather it is proportional to mass $\cdot$ length^2. Since leg length is the variable by which we scale our model, it did not make sense to run a linear regression on this parameter. The body masses, however, were empirically determined, not calculated with L. We ran a linear regression on the log-scaled body masses and found that the values from the literature scaled with $L^{2.64}$, rather than L^3, meaning the total inertia of the model scales with $L^{4.64}$. Substituting this scaling and our findings from the stiffness regression into Eq. (8), we find a natural frequency that scales with $\frac{1}{L^{0.87}}$, exactly what we see from the original linear regression run on the measured natural frequencies of the model. This confirms that our model scaling unexpectedly is due to the true mass of the species we tested scaling with $L^{2.64}$, not L^3.

What might account for the scaling difference? The notion that mass scales with length cubed was originally derived under the assumption that animals are roughly cylindrical in shape [14,22], which works well for larger animals. However, smaller animals tend to take on a much more crouched posture, which would affect the distribution of body mass and leg geometry [21]. This very different posture could affect the mass-to-leg length relationship and consequently lead it to deviate from the isometric L^3 scaling.

Frequency scaling aside, our model, before correction, may also underestimate stiffness by a factor of 28. There may be multiple reasons for this, but two primary causes are likely our model's inability to account for significant anatomical differences between species and musculature differences between the joints in a given leg. The 4-bar mechanism is modeled after a human standing with feet hip-width apart and isometrically scaled to the size of each animal. This means we do not account for changes in stance width, body center of mass location, or species-specific mass distributions, among other factors. It makes sense that stiffness for our cockroach-scaled model would be underestimated since cockroaches have a splayed-out stance, which should theoretically be more stable than the hip-width leg stance modeled. Additionally, we considered only rotational hip stiffnesses that apply torques linearly proportional to the angular

displacement. However, passive forces in biological muscles exhibit large transient effects and viscoelasticity, which may need to be reflected in future model interactions. Finally, joint stiffness data reported in literature and used in this work, typically comes from the knee joint, which for many species has less musculature than the hip joint. Cross sections of a cockroach coxa and femur, provided by Sasha Zill (personal communication), show there is roughly seven times more cross-sectional area in the muscles controlling the hip than the knee. Since joint stiffness is correlated to muscle size, this would further explain why our model underestimates stiffness. These findings highlight the importance of considering stance configuration, posture, biological material properties, and leg joint anatomy in future modeling efforts.

5 Conclusions and Future Work

In this work, we explored the relationship between an animal's natural frequency during stance and its passive stability. We theorized that when a creature's undamped natural frequency is larger than its walking cycle frequency, it has a passively stable stance. As a consequence, in response to perturbations, large animals, such as humans, require nervous system activity to remain stable [2], whereas small animals, such as cockroaches, maintain stability without additional neural activity [20]. Our initial model implementation, assuming mass scaled with L^3 and isometrically scaling the human-inspired four-bar mechanism, resulted in deviations from this prediction. However, further analysis found that this approach underestimated hip stiffness compared to reported values in the literature. Correcting this underestimation and re-running the simulations produced results supporting this claim. With the correction, when scaled for both cockroaches and fruit flies, the model exhibits higher natural frequencies than walking frequencies, while the opposite is true for larger animals like horses and humans. This supports the theory that, in small animals, the passive mechanics of the joint are fast enough to dampen perturbation without the aid of neuromuscular feedback.

While this is a promising result, there are still a few issues with this model that require further investigation. As stated previously, we needed to increase the stiffness of the hip joints by a factor of 28 to get the model stiffness for a cockroach to agree with the stiffness found in the literature [20]. However, we have not yet investigated whether this factor should be constant across all species. It is also possible that the stiffness multiplier may not be so large if we change the model to account for preferred stance widths and limb postures. Wider stances would naturally manifest a greater overall stiffness for the 4-bar mechanism, giving the cockroach model a stiffness closer to that found in the literature. As this is an ongoing project, both of these issues will be explored in future work

Acknowledgements. We would like to thank Dr. Alexander Hunt and Dr. Nicholas Szorcinski for their assistance with simulation troubleshooting and lending us their expertise on legged locomotion behavior for a large variety of animals. We would also like to thank Dr. Sasha Zill for sharing cross sections of a cockroach leg, which we used to verify the difference in musculature and stiffness for the knee and hip joints.

References

1. Audet, J., et al.: Control of forelimb and hindlimb movements and their coordination during quadrupedal locomotion across speeds in adult spinal cats. J. Neurotrauma **39**(15–16), 1113–1131 (2022). https://doi.org/10.1089/neu.2022.0042
2. Bingham, J.T., Choi, J.T., Ting, L.H.: Stability in a frontal plane model of balance requires coupled changes to postural configuration and neural feedback control. J. Neurophysiol. **106**(1), 437–448 (2011). https://doi.org/10.1152/jn.00010.2011
3. Delcomyn, F.: The locomotion of the cockroach Periplaneta Americana. J. Exp. Biol. **54**(2), 443–452 (1971). https://doi.org/10.1242/jeb.54.2.443
4. Demertzis, N., et al.: Effect of olive oil phenolics on lipidemic profile and oxidative stress in mice. Elyns Group - Journal of Food, Nutrition and Dietetics (2018)
5. Deng, K., Szczecinski, N., Arnold, D., Andrada, E., Fischer, M., Quinn, R., Hunt, A.J.: Neuromechanical model of rat hindlimb walking with two-layer cpgs. Biomimetics **4**(1), (2019). https://doi.org/10.3390/biomimetics4010021
6. Full, R., Ahn, A.: Static forces and moments generated in the insect leg: comparison of a three-dimensional musculo-skeletal computer model with experimental measurements. J. Exp. Biol. **198**, 1285–98 (1995). https://doi.org/10.1242/jeb.198.6.1285
7. Garcia, M., Kuo, A., Peattie, A.M., Wang, P., Full, R.: Damping and size: insights and biological inspiration (2000)
8. Ghasemi, A., Jeddi, S., Kashfi, K.: The laboratory rat: age and body weight matter. EXCLI J **20**, 1431–1445 (2021). https://doi.org/10.17179/excli2021-4072
9. Greene, E.C.: Anatomy of the rat. Trans. Am. Philos. Soc. **27**, iii–370 (1935). https://doi.org/10.2307/1005513
10. Grillner, S.: Locomotion in vertebrates: central mechanisms and reflex interaction. Physiol. Rev. **55**(2), 247–304 (1975). https://doi.org/10.1152/physrev.1975.55.2.247
11. Grillner, S., Halbertsma, J., Nilsson, J., Thorstensson, A.: The adaptation to speed in human locomotion. Brain Res. **165**(1), 177–82 (1979). https://doi.org/10.1016/0006-8993(79)90059-3
12. Guschlbauer, C., Scharstein, H., Buschges, A.: The extensor tibiae muscle of the stick insect: biomechanical properties of an insect walking leg muscle. J. Exp. Biol. **210**(6), 1092–1108 (2007). https://doi.org/10.1242/jeb.02729
13. Hajian, A.Z., Howe, R.D.: Identification of the mechanical impedance at the human finger tip. J. Biomech. Eng. **119**(1), 109–114 (1997). https://doi.org/10.1115/1.2796052
14. Hemmingsen, A.: Energy metabolism as related to body size and respiratory surface, and its evolution. Rep. Steno Meml. Hosp. **13**, 1–110 (1960)
15. Herbin, M., Hackert, R., Gasc, J.P., Renous, S.: Gait parameters of treadmill versus overground locomotion in mouse. Behav. Brain Res. **181**, 173–9 (2007). https://doi.org/10.1016/j.bbr.2007.04.001
16. Hildebrand, M.: Motions of the running cheetah and horse. J. Mammal. **40**(4), 481–495 (1959). https://doi.org/10.2307/1376265

17. Hooper, S.L.: Body size and the neural control of movement. Curr. Biol. **22**(9), R318–R322 (2012). https://doi.org/10.1016/j.cub.2012.02.048
18. Hooper, S.L., Guschlbauer, C., Blümel, M., Rosenbaum, P., Gruhn, M., Akay, T., Büschges, A.: Neural control of unloaded leg posture and of leg swing in stick insect, cockroach, and mouse differs from that in larger animals. J. Neurosci. **29**(13), 4109–19 (2009). https://doi.org/10.1523/JNEUROSCI.5510-08.2009
19. Hruska, R.E., Kennedy, S., Silbergeld, E.K.: Quantitative aspects of normal locomotion in rats. Life Sci. **25**(2), 171–179 (1979). https://doi.org/10.1016/0024-3205(79)90389-8
20. Jindrich, D.L., Full, R.J.: Dynamic stabilization of rapid hexapedal locomotion. J. Exp. Biol. **205**(18), 2803–2823 (2002). https://doi.org/10.1242/jeb.205.18.2803
21. JR, U.: Constraints on muscle performance provide a novel explanation for the scaling of posture in terrestrial animals. Biol Lett **9**(4), (2013). https://doi.org/10.1098/rsbl.2013.0414
22. McMahon, T.: Size and shape in biology. Science **179**(4079), 1201–1204 (1973). https://doi.org/10.1126/science.179.4079.1201
23. Merlet, A.N., et al.: Sensory perturbations from hindlimb cutaneous afferents generate coordinated functional responses in all four limbs during locomotion in intact cats. eNeuro **9**(6), (2022). https://doi.org/10.1523/ENEURO.0178-22.2022
24. Rao, S.: Mechanical Vibrations. No. v. 978, nos. 0-212813 in Mechanical Vibrations. Prentice Hall (2011). https://books.google.com/books?id=TOpBswEACAAJ
25. Smith, W., Thomas, J., Liu, J., Li, T., Moran, T.: From fat fruitfly to human obesity. Physiol. Behav. **136**, 15–21 (2014). https://doi.org/10.1016/j.physbeh.2014.01.017
26. Stark, H., Fischer, M.S., Hunt, A., Young, F., Quinn, R., Andrada, E.: A three-dimensional musculoskeletal model of the dog. Sci. Rep. **11**(1), (2021). https://doi.org/10.1038/s41598-021-90058-0
27. Stein, R., Zehr, E., Lebiedowska, M., Popović, D., Scheiner, A., Chizeck, H.: Estimating mechanical parameters of leg segments in individuals with and without physical disabilities. IEEE Trans. Rehabil. Eng. **3**, 201–11 (1996). https://doi.org/10.1109/86.536776
28. Sutton, G.P., Szczecinski, N.S., Quinn, R.D., Chiel, H.J.: Phase shift between joint rotation and actuation reflects dominant forces and predicts muscle activation patterns. PNAS Nexus **2**(10), pgad298 (2023). https://doi.org/10.1093/pnasnexus/pgad298
29. Tan, G.R., Raitor, M., Collins, S.H.: Bump'em: an open-source, bump-emulation system for studying human balance and gait. In: 2020 IEEE International Conference on Robotics and Automation (ICRA), pp. 9093–9099 (2020). https://doi.org/10.1109/ICRA40945.2020.9197105
30. Vasudevan, E.V.L., Hamzey, R.J., Kirk, E.M.: Using a split-belt treadmill to evaluate generalization of human locomotor adaptation. J. Vis. Exp. (126), (2017). https://doi.org/10.3791/55424
31. Weiss, P., Hunter, I., Kearney, R.: Human ankle joint stiffness over the full range of muscle activation levels. J. Biomech. **4**, 539–44 (1988). https://doi.org/10.1016/0021-9290(88)90217-5
32. Williams, S.B., Wilson, A.M., Rhodes, L., Andrews, J., Payne, R.C.: Functional anatomy and muscle moment arms of the pelvic limb of an elite sprinting athlete: the racing greyhound (canis familiaris). J. Anat. **213**(4), 361–372 (2008). https://doi.org/10.1111/j.1469-7580.2008.00961.x

33. Witte, H., Biltzinger, J., Hackert, R., Schilling, N., Schmidt, M., Reich, C., Fischer, M.S.: Torque patterns of the limbs of small therian mammals during locomotion on flat ground. J. Exp. Biol. **205**(9), 1339–1353 (2002). https://doi.org/10.1242/jeb.205.9.1339
34. Wosnitza, A., Bockemühl, T., Dübbert, M., Scholz, H., Büschges, A.: Inter-leg coordination in the control of walking speed in Drosophila. J. Exp. Biol. **216**(3), 480–491 (2013). https://doi.org/10.1242/jeb.078139
35. Zakotnik, J., Matheson, T., Dürr, V.: Co-contraction and passive forces facilitate load compensation of aimed limb movements. J. Neurosci. **26**(19), 4995–5007 (2006). https://doi.org/10.1523/JNEUROSCI.0161-06.2006